Journal of Macromolecular Science, Part A
Publication details, including instructions for authors and subscription information:
http://www.informaworld.com/smpp/title~content=t713597274

Synthesis and Characterization of H-bonded Side-Chain Liquid-Crystalline Polysiloxanes

Fan-Bao Meng[a]; Yong-Mei Gao[a]; Bao-Yan Zhang[a]; Xiao-Xu Xu[a]
[a] Research Center for Molecular Science and Engineering, Northeastern University, Shenyang, P. R. China

To cite this Article Meng, Fan-Bao , Gao, Yong-Mei , Zhang, Bao-Yan and Xu, Xiao-Xu(2008) 'Synthesis and Characterization of H-bonded Side-Chain Liquid-Crystalline Polysiloxanes', Journal of Macromolecular Science, Part A, 45: 2, 186 — 194
To link to this Article: DOI: 10.1080/10601320701787008
URL: http://dx.doi.org/10.1080/10601320701787008

Journal of Macromolecular Science®, Part A: Pure and Applied Chemistry (2008) **45**, 186–194

ISSN: 1060-1325 print/1520-5738 online
DOI: 10.1080/10601320701787008

Synthesis and Characterization of H-bonded Side-Chain Liquid-Crystalline Polysiloxanes

FAN-BAO MENG, YONG-MEI GAO, BAO-YAN ZHANG, and XIAO-XU XU

Research Center for Molecular Science and Engineering, Northeastern University, Shenyang, P. R. China

Received January, 2007, Accepted August, 2007

Smectic Liquid-crystalline (LC) polysiloxanes **P1** ∼ **P7** were prepared using cholesteryl 6-undec-10-enoyloxy-naphthalene-2-carboxylate and cholesteryl 3-sulfo-4-undec-10-enoyloxy-benzoate in a one-step reaction with sulfonic acid group contents ranging between 0 and wt 4.39%. With an increase of sulfonic acid groups, the glass transition temperature rose slightly; while the temperature of clear point decreased. As sulfonic groups increased, H-bonding interaction strengthened, resulting in an increase of glass transition temperature. On the other hand, aggregates of H-bond derived from sulfonic acids would destroy the homogeneous rigid moieties and the high-ordered structure, resulting in a temperature of clear point decreased. In X-ray measurement, all the polymers displayed sharp strong peaks around $2\theta \approx 2.6^\circ$ and broad peaks around $2\theta \approx 16.6^\circ$. The broad peaks at wide-angle are similar, but there is great different at low angles. For the polymer without sulfonic acid, the only one strong peak at low angle indicates high-ordered lamellar structure due to homogeneous rigid moieties. For the polymers containing more sulfonic acid, two sharp peaks appeared at low angles, and the intensities of these two peaks varied. With increase of sulfonic acid groups in the polymer systems, the hydrogen-bonding aggregates in domains would divide the homogeneous rigid mesogens into two kinds of nanophases, that is, one containing non H-bond mesogens and another involving H-bonding aggregated mesogens. These two different nanophases result in different lamellar spacings.

Keywords: liquid-crystalline polymers (LCP); polysiloxanes; H-bond; phase behavior

1 Introduction

Recently, self-assembled phenomena through the molecular recognition between individual constituents have been explored in various areas. Hydrogen bonding is one of the most important key factors for the molecular recognition in nature (1). Hydrogen bonding has been discussed extensively in the literature during the past five decades. There are several monographs and hundreds of papers that dealt with hydrogen bonding. A large number of supramolecular liquid crystals have been built based on hydrogen bonding interaction to date. Supramolecular main-chain liquid-crystalline polymers (LCPs), side-chain mesogenic polymers as well as network, and low molecular weight complexes have been prepared through intermolecular H bonds (2–10).

A great variety of hydrogen bonds have been used to build the supramolecular mesogenic structures. Most of the supramolecular H-bonded liquid-crystalline complexes are due to hetero-intermolecular hydrogen-bonding interaction derived from two complementary different monomers with a proton donor and a proton acceptor, including carboxylic acid/pyridine (11), uracil/2,6-diaminopyridine (12) and phenol/tertiary amine (13), etc. There are also some examples of the liquid crystals formed by identical molecules through homo-intermolecular hydrogen bonds. For example, some carboxylic acids dimerize through intermolecular hydrogen bonds and thus induce liquid crystallinity (14, 15). Other H-bonded liquid-crystalline examples were also reported by identical amphiphilic species, such as carbohydrates (16), polyols (17), etc.

In the synthesis of H-bonded LCPs, mesogenic constituents are frequently used although it is not a prerequisite (18). An example of a non-mesogenic precursor may be found in mixtures of functional vinyl polymers and mutually reactive non-liquid-crystalline rigid aromatic derivatives, with no flexible spacer (or only a very short one) between the constitutive components (19).

For liquid crystals, the phase behavior is governed by the shape and size of their molecular constituents and a delicate balance of noncovalent intermolecular interactions (20). Hydrogen bonding has been used to force the formation of molecular aggregates with liquid-crystal properties. Therefore, it is necessary to investigate the effect of hydrogen bonding on the properties of liquid-crystal phases. Compared

Address correspondence to: Bao-Yan Zhang, Research Center for Molecular Science and Engineering, Northeastern University, Shenyang 110004, P. R. China. Tel.: +86 24 83687671; E-mail: byzcong@163.com

with weak polar groups such as carboxylic acid, carbohydrates and polyols, sulfonic acid is a strong polar acid, inducing strong hydrogen-bonding interaction. It is interesting to study the effect of sulfonic acid hydrogen-bonding on phase behavior and mesomorphic properties of LCPs.

In a previous report, we synthesized a series of side-chain LCPs by use of a cholesteryl monomer and a non-cholesteryl monomer containing sulfonic acid (21). In order to investigate better the effect of hydrogen bonding derived from sulfonic acid on the liquid crystal properties, now we synthesized sulfonic acid-containing side-chain LCPs with both monomers containing cholesteryl groups.

2 Experimental

2.1 Materials and Measurements

10-Undecylenoic acid, cholesterol, 6-hydroxy-naphthalene-2-carboxylic acid, p-hydroxybenzoic acid, potassium hydroxide, sulfuric acid and hexachloroplatinic acid hydrate were obtained from Jilin Chemical Industry Company and used without any further purification. Poly(methylhydrogeno)-siloxane (PMHS) was provided by Merk. Pyridine, thionyl chloride, toluene, ethanol, chloroform, tetrahydrofuran (THF) and methanol were purchased from Shenyang Chemical Co. Pyridine was purified by distillation over KOH and NaH before using.

The element analyses (EA) were carried out by using an Elementar Vario EL III (Elementar, Germany). FTIR spectra of the synthesized polymers and monomers in solid state were obtained by the KBr method performed on a Perkin-Elmer instruments Spectrum One Spectrometer (Perkin-Elmer, Foster City, CA). ^{1}H-NMR (300 MHz) spectra were obtained with a Varian Gemini 300 NMR Spectrometer (Varian Associates, Palo Alto, CA) with Fourier transform with dimethyl sulfoxide-d_6 (DMSO-d_6) or $CDCl_3$ as a solvent and tetramethylsilane (TMS) as an internal standard. X-ray measurements of the samples were performed using Cu Kα ($\lambda = 1.542$ Å) radiation monochromatized with a Rigaku DMAX-3A X-ray diffractometer (Rigaku, Japan). Thermal transition properties were characterized by a NETZSCH instruments DSC 204 (Netzsch, Wittelsbacherstr, Germany) at a heating rate of 10°C min^{-1} under nitrogen atmosphere. Phase transition temperatures were collected during the second heating and the first cooling scans. Visual observation of liquid crystalline transitions and optical textures under cross polarized light was made by a Leica DMRX (Leica, Wetzlar, Germany) POM equipped with a Linkam THMSE-600 (Linkam, Surrey, England) hot stage.

2.2 Synthesis of Cholesteryl 6-Undec-10-enoyloxy-naphthalene-2-carboxylate (M1).

Synthesis routes of **M1** were shown in Figure 1a. 6-Hydroxy-naphthalene-2-carboxylic acid (48.9 g, 0.26 mol) and 260 mL pyridine were added into a round flask equipped with a reflux line. The solution was stirred at room temperature and added dropwise with 10-undecenoyl chloride (**1**) (52.7 g, 0.26 mol) which was prepared according to a previously reported synthetic method (22). The reaction mixture was stirred at 85°C for 24 h. After cooling to room temperature, the mixture was poured into 1000 mL cold water and acidified with 6 N sulfuric acid. The precipitates were isolated by filtration and dried in a vaccum oven. Recrystallization in

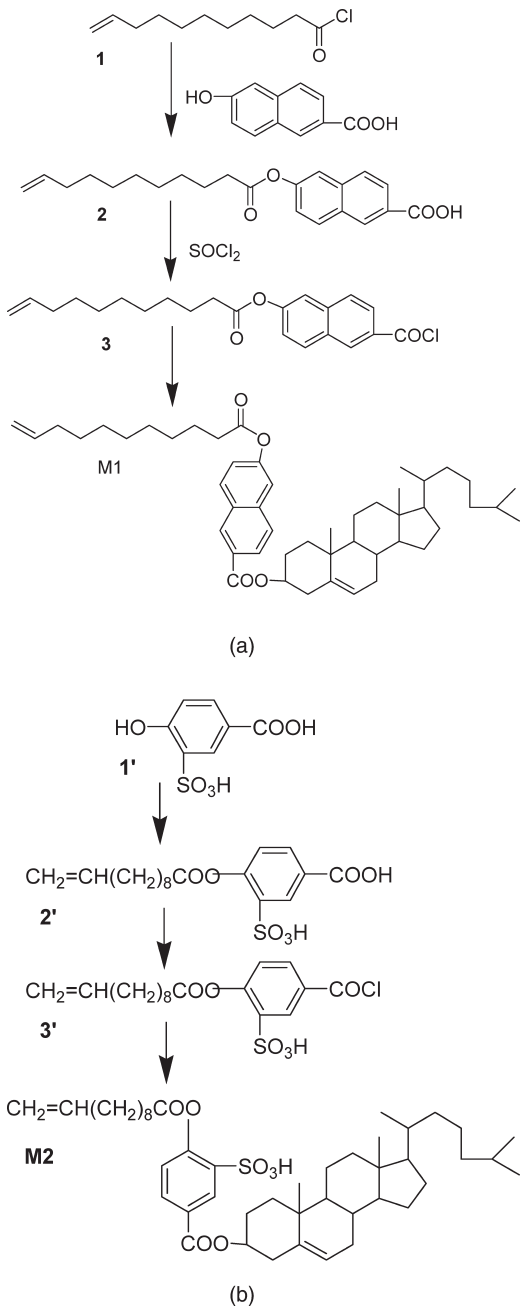

Fig. 1. Synthesis routes of the liquid crystalline monomer (a) cholesteryl 6-undec-10-enoyloxy-naphthalene-2-carboxylate (**M1**) and (b) cholesteryl 3-sulfo-4-undec-10-enoyloxy-benzoate (**M2**).

ethanol results in yellow crystals of 6-undec-10-enoyloxy-naphthalene-2-carboxylic acid (**2**).

Yield: 92%. m.p.: 158°C. IR (KBr, cm^{-1}): 3056, 2928, 2856 (-CH_2-, CH_2= and =CH), 2605–2501 (-OH in -COOH), 1748 (C=O in ester linkage), 1689 (C=O in -COOH) 1602, 1493 (Ar), 1276 (C-O-C). ^{1}H-NMR (DMSO-d_6, δ, ppm): 1.24–2.11 [m, 12H, CH_2=CHCH_2(CH_2)$_6$$CH_2$COO-], 2.66–3.01 (m, 4H, CH_2=CHCH_2(CH_2)$_6$CH_2COO-), 5.54–5.77 (t, 2H, CH_2=CH-), 6.09–6.18 (m, 1H, CH_2=C*H*-), 6.98–8.13 (m, 6H, Ar-*H*), 10.31 (s, 1H, -COO*H*).

The intermediate **2** (37.3 g, 0.1 mol), 100 mL thionyl chloride and 2.0 mL of pyridine were added into a round flask equipped with an absorption instrument of hydrogen chloride. The mixture was stirred at room temperature for 3 h, then heated to 60°C and kept for 10 h in a water bath to ensure that the reaction finished. The excess thionyl chloride was distilled under reduced pressure. Then, 100 mL cold chloroform was added to the residue at 20°C to obtain chloroform solution of 6-chlorocarbonyl-naphthalene-2-yl undec-10-enoate (**3**).

Sodium carbonate (10.6 g, 0.1 mol), cholesterol (38.7 g, 0.1 mol) and 200 mL chloroform were added into a round flask equipped with a reflux line. The solution of **3** was added dropwise to the reaction mixture at room temperature. Then, the reaction solution was heated, stirred at 60°C for 16 h, and filtered. Some chloroform was distilled out from the filter liquor, and the residue was poured into 200 mL cold ethanol. The precipitates were isolated by filtration and dried in a vaccum oven. Recrystallization in acetone results in white crystals of cholesteryl 6-undec-10-enoyloxy-naphthalene-2-carboxylate (**M1**).

Yield: 83%. m.p.: 90°C. IR (KBr, cm^{-1}): 2957, 2925, 2859 (CH_3- and -CH_2-), 1746, 1725 (C=O in different ester linkage), 1605, 1499 (Ar), 1291 (C-O-C). Anal. calcd. for $C_{49}H_{70}O_4$: C, 81.39%; H, 9.76%. Found: C, 81.22%; H, 9.82%. ^{1}H-NMR ($CDCl_3$, δ, ppm): 0.82–2.19 (m, 53H, R-C*H*), 2.62–2.98 (m, 6H, CH_2=CHCH_2(CH_2)$_6$CH_2COO- and -CH_2- in cholesteryl), 4.23–4.58 (m, 1H, -O-C*H*- in cholesteryl), 5.48–5.70 (t, 2H, CH_2=CH-), 6.01–6.20 (m, 2H, CH_2=C*H*- and =C*H*- in cholesteryl groups), 7.21–8.43 (m, 6H, Ar-*H*).

2.3 Synthesis of Cholesteryl 3-Sulfo-4-undec-10-enoyloxy-benzoate (M2)

Synthesis routes of **M2** were shown in Figure 1b. 4-Hydroxy-3-sulfo-benzoic acid (**1′**) was synthesized according to a reported procedure (23). Compound **1′** (21.8 g, 0.10 mol) was dissolved in 160 mL pyridine to form a solution. 10-undecenoyl chloride (20.2 g, 0.1 mol) was added dropwise to the solution and reacted at 80°C for 28 h. The mixture was cooled, poured in 200 mL of cold water and acidified with a 6 N sulfuric acid solution. The precipitates were isolated by filtration and dried in a vaccum oven. Recrystallization in ethanol results in brown crystals of 3-sulfo-4-undec-10-enoyloxy-benzoic acid (**2′**).

Yield: 72%. m.p.: 182°C. IR (KBr, cm^{-1}): 3437 (-OH in -SO_3H), 3053, 2921, 2850 (-CH_2-, CH_2= and =CH), 2608–2511 (-OH in -COOH), 1750 (C=O in ester linkage), 1691 (C=O in -COOH), 1603, 1499 (Ar), 1278 (C-O-C), 1231–1033 (S=O). ^{1}H-NMR (DMSO-d_6, δ, ppm): 1.12–2.18 [m, 12H, CH_2=CHCH_2(CH_2)$_6$$CH_2$COO-], 2.57–2.93 (m, 4H, CH_2=CHCH_2(CH_2)$_6$CH_2COO-), 5.49–5.69 (t, 2H, CH_2=CH-), 5.99–6.18 (m, 1H, CH_2=C*H*-), 7.46–8.63 (m, 3H, Ar-*H*), 10.32 (s, 1H, -COO*H*), 11.19 (s, 1H, -SO_3*H*).

The intermediate **2′** (21.5 g, 0.056 mol), 80 mL thionyl chloride and 1.0 mL of pyridine were added into a round flask equipped with an absorption instrument of hydrogen chloride. The mixture was stirred at room temperature for 3 h, then heated to 60°C and kept for 24 h in a water bath to ensure that the reaction finished. The excess thionyl chloride was distilled under reduced pressure. Then 100 mL cold chloroform was added to the residue at 20°C to obtain chloroform solution of 4-chlorocarbonyl-2-sulfo-phenyl undec-10-enoate (**3′**).

Cholesterol (21.6 g, 0.056 mol) and 30 mL chloroform was dissolved in 60 mL pyridine to form a solution. The chloroform solution of **3′** was added dropwise to the solution and reacted at 60°C for 31 h; then the chloroform was distilled out. The mixture was cooled, poured in 200 mL of cold water and acidified with 6 N sulfuric acid solution. The precipitated crude product was filtered, dried overnight under vacuum to obtain a yellow powder of cholesteryl 3-sulfo-4-undec-10-enoyloxy-benzoate (**M2**).

Yield: 67%. m.p.: 112°C. IR (KBr, cm^{-1}): 3467 (-O-H), 2956, 2920, 2863 (CH_3- and -CH_2-), 1745, 1729 (C=O), 1605, 1501 (Ar), 1291 (C-O-C). Anal. Calcd for $C_{45}H_{68}O_7S$: C, 71.77%; H, 9.10%; S, 4.26%. Found: C, 71.65%; H, 9.02%; S, 4.24%. ^{1}H-NMR (DMSO-d_6, δ, ppm): 0.92–2.28 (m, 53H, R-C*H*), 2.61–2.92 (m, 6H, CH_2=CHCH_2(CH_2)$_6$-CH_2COO- and -CH_2- in cholesteryl), 4.26–4.64 (m, 1H, -O-C*H*- in cholesteryl), 5.46–5.71 (t, 2H, CH_2=CH-), 6.01–6.22 (m, 2H, CH_2=C*H*- and =C*H*- in cholesteryl groups), 7.31–8.70 (m, 3H, Ar-*H*), 11.12 (s, 1H, -SO_3*H*).

2.4 Synthesis of the Polymers

For synthesis of polymers **P1**-**P7**, the same method was adopted. The polymerization experiments, yield and solubility properties were summarized in Table 1. The synthesis of polymer **P3** was given as an example. Liquid-crystalline monomer **M1** (2.98 g, 4.13 mmol) was dissolved in 80 mL of dry, fresh distilled chloroform. To the stirred solution, liquid crystalline monomer **M2** (0.28 g, 0.37 mmol), poly(methylhydrogeno)siloxane (PMHS, 0.32 g, 0.15 mmol) and 2 mL of H_2PtCl_6/THF (0.50 g hexachloroplatinic acid hydrate dissolved in 100 mL tetrahydrofuran THF) were added and heated under nitrogen and anhydrous conditions at 60°C for 48 h. The solvent was removed under reduced pressure, and the crude polymer was purified by precipitation from solution in methanol by the addition of THF. After filtration and evaporation of the solvent, the product was dried at 80°C for 2 h under vacuum to obtain 3.22 g of polymer in the yield of 90%.

Table 1. Polymerization, yield, sulfonic acid content and solubility of the polymers

Sample	Feed PMHS (mmol)	**M1** (mmol)	**M2** (mmol)	Sulfonic acid[a] (wt%)	Yield (%)	Solubility[b]	
						Toluene	Chloroform
P1	0.15	4.5	0	0	91	+++++	+++++
P2	0.15	4.38	0.12	0.21	93	+++++	+++++
P3	0.15	4.13	0.37	0.64	90	++++	+++++
P4	0.15	3.75	0.75	1.27	91	+++	++++ +
P5	0.15	3.25	1.25	2.11	90	++	+++++
P6	0.15	2.63	1.87	3.16	92	++	+++++
P7	0.15	1.88	2.62	4.39	90	+	+++++

[a]Mass fraction of sulfonic acid group calculated via EA of S element on the polymer systems.
[b]The more +, the better solubility in solvent.

3 Results and Discussion

3.1 Syntheses

The synthetic routes for the target liquid crystalline monomers are shown in Figure 1. All the monomers **M1** and **M2** were obtained through the reaction of relevant acyl chloride and cholesterol in appropriate reactive solvent at a reasonable temperature. The chemical structures of the monomers were characterized by use of EA, IR, and ^{1}H-NMR spectra, which was in good agreement with the prediction. The spectra of **M1** and **M2** suggest that the purity is high and this was confirmed by EA. IR spectra of **M1** showed characteristic bands at 1746, 1725, and 1605–1499 cm^{-1} attributable to different ester C═O, and aromatic C═C stretching bands, respectively. ^{1}H-NMR spectra of **M1** showed peaks at 8.43–7.21, 6.20–5.48, and 2.98–0.82 ppm corresponding to aromatic protons, olefinic protons, methyl and methylene protons, respectively. IR spectra of **M2** showed characteristic bands at 3467, 1745–1729 and 1605–1501 cm^{-1} attributable to hydroxyl group, ester C═O, and aromatic C═C stretching bands, respectively. For organic sulfonic acid, the FTIR absorption range of the O═S═O asymmetric and symmetric stretching modes lies in 1100 $\sim$ 1260 and 1010 $\sim$ 1080 cm^{-1}, respectively. Because of the overlap found for both asymmetric and symmetric stretching bands of S═O with C-O stretching bands under study, it is difficult to identify S═O of sulfonic acid in **M2** by use of IR spectra. EA and ^{1}H-NMR spectra were employed for characterization of sulfonic acid groups in **M2**. ^{1}H-NMR spectra of **M2** showed peaks at 11.12, 8.70–7.31, 6.22–5.46, and 2.28–0.92 ppm corresponding to sulfonic acid protons, aromatic protons, olefinic protons, and methyl and methylene protons, respectively.

The polymers were synthesized through a hydrosilylation reaction. The solubility of the obtained polymers decreased with increase of sulfonic acid groups in toluene, but didn't change greatly in chloroform, as listed in Table 1. As shown in the IR spectra of the polymers **P1**–**P7**, the disappearance of the Si-H stretching at 2160 cm^{-1} indicates successful incorporation of monomers into the polysiloxane chains (21). In addition, the characteristic ester C═O absorption bands in corresponding monomers and the characteristic Si-O-Si broad stretching bands at 1300–1000 cm^{-1} appeared in all the polymers. Polymer **P3** contains the representative features for all of the liquid-crystalline polymers, their characteristic absorption bands are as follows: 3496–3444 cm^{-1}(O-H stretching in sulfonic acid groups), 2946–2850 cm^{-1} (C-H aliphatic), 1746–1722 cm^{-1} (C═O stretching in different kinds of ester modes), 1605, 1509 cm^{-1} (aromatic stretching). In order to characterize mass percentage of sulfonic acid groups in the polymer systems, the measurements of EA were employed to determine S element, and the corresponding sulfonic acid contents were listed in Table 1. It showed that the mass percentage of sulfonic acid groups increased with increase of monomer **M2** in the polymers.

3.2 Liquid-Crystalline Properties of Monomers

The mesomorphic properties of **M1** and **M2** were investigated with DSC and POM. Their phase transition temperatures and corresponding enthalpy changes are summarized in Table 2.

For monomer **M1**, during heating scans, a melting transition and a cholesteric-to-isotropic phase transition appeared at 90.3°C and 251.2°C, respectively; an isotropic-to-cholesteric phase transition and crystallization temperature appeared during cooling scans at 239.6°C and 89.1°C, respectively. Observed by POM, **M1** exhibited an enantiotropic cholesteric texture upon heating and cooling, and the representative optical textures were displayed in Figure 2. When **M1** was heated above 90°C, the sample began to melt, and mesomorphic properties appeared; a typical oily streak texture of the cholesteric phase gradually appeared. Some of the oily streaks appeared in bundles, as shown in Figure 2a. The director is basically anchored under planar conditions at the substrates, i.e., with the long molecular axis parallel to the bounding plates, which implies that the cholesteric helix axis is oriented perpendicular to the glass plates. On cooling, the isotropic-cholesteric transition was accomplished via nucleation and growth of spherical cholesteric domains within the isotropic melt. At a later

Table 2. Liquid-crystalline properties of monomers **M1** and **M2**

Monomers	Transition temperature[a,b] in °C (corresponding enthalpy changes in $J \cdot g^{-1}$)	ΔT_1^c	ΔT_2^d
M1	Heating: K 90.3 (45.60) Ch 251.2 (2.13) I Cooling: I 239.6 (2.02) Ch 89.1 (23.92) K	160.9	150.5
M2	Heating: K 112.2 (52.91) S_A 143.1 (4.23) Ch 221.0 (0.88) I Cooling: I 215.3 (0.89) Ch 132.1 (3.65) S_A 98.9 (23.13) K	108.8	116.4

[a]K solid, Ch cholesteric, S_A smectic A, I isotropic.
[b]Peak temperatures were taken as the phase transition temperature.
[c]Mesophase temperature ranges on heating cycle.
[d]Mesophase temperature ranges on cooling cycle.

point these domains coalesce (as depicted in Figure 2b) and eventually the cholesteric texture completely filled the microscope field of view. The phenomenon of selective reflection was not seen by naked eye. These suggest the liquid crystalline monomer **M1** should be a kind of long pitch cholesterics (24).

Monomer **M2** showed a melting transition at 112.2°C, a smectic-to-cholesteric transition at 143.1°C and a cholesteric-to-isotropic phase transition at 221.0°C on heating cycles. During cooling scans, an isotropic-to-cholesteric transition at 215.3°C, a cholesteric-to-smectic transition at 132.1°C and crystallization at 98.9°C were observed. Observed by POM, **M2** exhibited different smectic textures and cholesteric textures. The representative optical textures of the LC monomer **M2** were displayed in Figure 3. When **M2** was heated above 112°C, the sample began to melt, and a fan-shaped texture of smectic A phase gradually appeared. When the sample was heated continuously, some fans deformed and disappeared, and some oily streaks emerged meanwhile, as shown in Figure 3a. On cooling, a fan-like texture was observed within individual fans the helix axis (equivalent to the optic axis) was oriented uniformly, as depicted in Figure 3b. These kinds of fan-like textures are displayed for strongly twisted materials, and

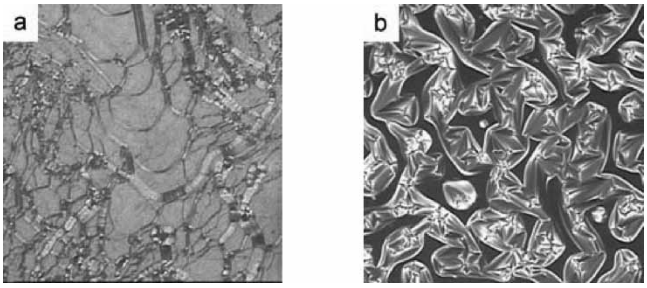

Fig. 2. Optical texture of monomer **M1** (200×): (a) oily streak texture at heating to 245°C; (b) coalescence of the cholesteric droplets at cooling to 236°C.

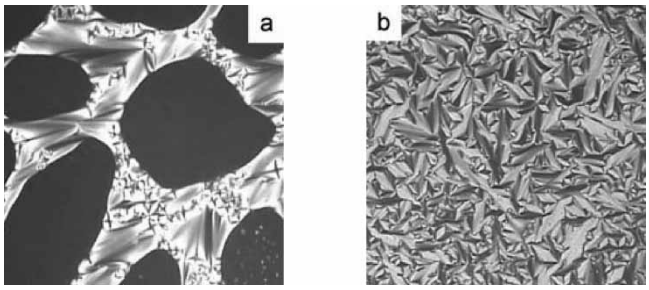

Fig. 3. Optical texture of monomer **M2** (200×): (a) coexistence of fan-shaped textures with some oily streaks at heating to 210°C; (b) fan-like texture of a short pitch cholesteric phase at cooling to 143°C.

can be very similar to those observed in SmA phase (24). In comparison with a long pitch structure of **M1,** this cholesteric phase of **M2** suggests a short pitch structure due to H-bonding interaction derived from sulfonic acid groups in **M2**.

3.3 Thermal Properties of Polymers

For the polymers, Figure 4 shows the DSC thermograms of representative polymers synthesized, and the data are listed in Table 3. In the DSC thermograms, all the polymers **P1** ∼ **P7** revealed a glass transition at low temperature and smectic to isotropic transition at high temperature. Reversible mesomorphic phase transitions for all the polymers were observed because of enough LC molecular motion and orientation, although physical crosslinking of H-bonding derived from sulfonic acid containing mesogens disturbs some LC order of the polymer systems. From the data listed in Table 3, H-bonding derived from sulfonic acid in **P2** ∼ **P7** affected both glass transition and isotropic transition of the polymers. This results show some difference from our previous report (21), because these polymers are synthesized by use of two kinds of cholesteryl monomer with similar chemical structures except for sulfonic groups. With an increase of sulfonic acid groups in the polymers **P1** ∼ **P7**, the glass transition temperature rise slightly; while the temperature of clear point decreased, leading to mesophase

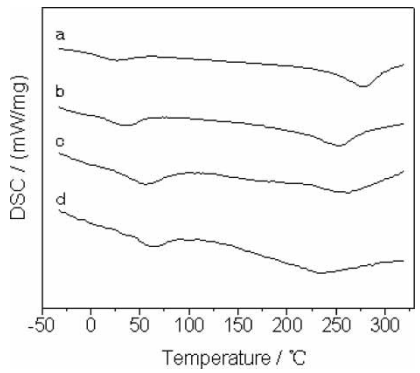

Fig. 4. DSC thermograms of the polymers on the second heating (10°C min^{-1}) for (a) **P1**; (b) **P3**; (c) **P5** and (d) **P7**.

Table 3. DSC and X-ray results of the series of polymers

	DSC				*2θ*		
Polymer	T_g (°C)	T_i (°C)	ΔH_i (J/g)	ΔT [a] (°C)	(°)	(°)	(°)
P1	27.0	278.4	2.32	251.4	2.51	—	16.61
P2	32.1	260.2	2.38	228.1	2.50	—	16.58
P3	36.9	252.8	2.46	215.9	2.51[b]	2.67	16.59
P4	46.2	252.1	2.21	205.9	2.51[b]	2.68	16.62
P5	58.7	256.7	1.89	198.0	2.50	2.67	16.59
P6	60.1	244.6	1.73	184.5	2.51	2.68[b]	16.61
P7	62.6	237.7	1.64	175.1	2.50	2.67[b]	16.58

[a]Mesophase temperature ranges (T_i—T_g).
[b]Stronger peaks between the two small angles.

temperature ranges decrease, as shown in Figure 5. For **P2** and **P3** with a little sulfonic acid in the polymer systems, the T_i decreased greatly, but it decreased slightly for the other polymers. Besides, the peaks of mesomorphic-isotropic transition in Figure 4 became weak and broad as sulfonic acid increases in the polymer systems, showing decrease of enthalpy change values (ΔH_i).

For the disordered systems of the atactic siloxane polymers, low temperatures induce vitrification rather than crystallization (25). For a polymer of this type, the glass-transition temperature may be considered as a measure of the backbone flexibility. In our case, the polysiloxanes were graft copolymerized via hydrosilylation reaction with PMHS and two monomers containing undecylenate groups. The space groups between polysiloxane main-chains and the mesogens are similar for all the polymers. Furthermore, both the monomers contain cholesteryl groups, leading to similar sterically hindered effect of all the polymers. Therefore, the backbone flexibility of the polymers is influenced mainly by H-bonding interaction derived sulfonic acid groups. As sulfonic groups increased in the polymer systems, H-bonding interaction strengthened, resulting in increase of glass transition temperature.

On the other hand, liquid crystalline polymers are most commonly composed of flexible and rigid moieties, self-assembly and nanophase separation (often lamellar for side chain architecture) occur frequently due to geometric and chemical dissimilarity of the two moieties. For **P1** which was prepared from **M1** and PMHS, it was easy to form a high-ordered lamellar structure because of homogeneous rigid moieties in the soft polymer matrix. These cause comparatively high T_i and ΔH_i. When some sulfonic mesogens were introduced into the polymer systems, H-bond derived from sulfonic acids would aggregate, thus the homogeneous rigid moieties and the high-ordered lamellar structure would be destroyed, resulting in T_i decreased greatly for **P2**. With an increase of sulfonic acid mesogens in the polymer systems, the hydrogen-bonding aggregates in domains would disturb LC molecular mobility and orientation, leading to decrease temperature of mesomorphic-isotropic transition and ΔH_i for other polymers. Furthermore, because the polymer systems contain growing aggregates owing to strong hydrogen-bonding interaction with increase of sulfonic acid-containing mesogens, the rigid moieties in the mesophase should consist of two parts: one comprises mesogens without H-bond component and another involves H-bonding aggregated mesogens. Thus more nanophase separation would be observed in the relatively nonpolar matrix.

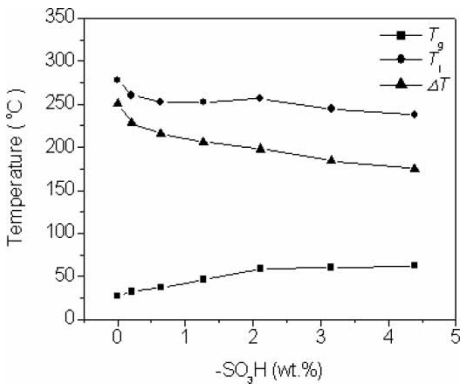

Fig. 5. Effect of sulfonic acid group mass fraction on phase transition temperatures of polymers.

3.4 Optical Texture of Polymers

The optical textures of the LC polymers are observed by use of polarizing optical microscope (POM) with hot stage under nitrogen atmosphere. POM observation combined with X-ray measurements showed that all the polyemrs exhibited enantiotropic smectic phase during heating and cooling cycles, which agrees with DSC thermograms.

The representative optical textures of the polymers are shown in Figure 6. Although all the monomers displayed cholesteric phase, all the chiral polymers didn't exhibit cholesteric phase textures, the reason for which, the polymer chains hinder the formation of the helical supermolecular structure of the mesogens. Furthermore, typical fan-shaped texture of smectic phase like small molecule **M2** didn't appear as well for all the polymers when they were heated and cooled, owing to the fact that the polymer skeletons restrict arrangement and

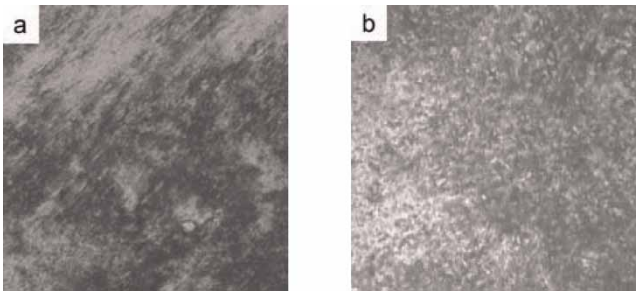

Fig. 6. Optical texture of polymers (200×): (a) texture of polymer **P1** at heating to 178°C; (b) texture of polymer **P5** at heating to 225°C.

flow of the mesogens. However, there is some difference between the textures of **P1** and the other polymers.

When the sample **P1** was heated above 27°C, eyesight became bright and LC textures appeared. The textures became obvious as the sample was heated continuously (see Figure 6a). The textures didn't change greatly until the sample was heated to T_i. For the chiral LCPs **P2**-**P7** containing more sulfonic acid groups, similar optical textures were exhibited. When the sample **P5** was heated above 58°C, the textures were similar to those of **P1**, but when it was heated continuously, some microstructure enlarged, and some aggregated blocks texture appeared, as shown in Figure 6b. In our case, the growing aggregates are attributed to strong hydrogen-bonding interaction among sulfonic mesogens in the polymer systems.

3.5 X-ray Diffraction of Polymers

The smectic nature of the LC phase and effect of sulfonic-acid containing mesogens on liquid-crystalline properties of the polymers are also characterized by X-ray analysis. Some representative X-ray profiles of series of polymers are shown in Figure 7. For all the polymer**s**, sharp strong peaks and broad peaks appear respectively at low angle around $2\theta \approx 2.6^\circ$ and wide-angle around $2\theta \approx 16.6^\circ$ in the X-ray profiles, and the data were listed in Table 3. The broad peaks of all the polymers appeared around $2\theta \approx 16.6^\circ$ are similar, and they are not at $2\theta \approx 20^\circ$ for **P1**-**P7,** suggesting chiral structure between two neighbor LC molecules within the layers of the mesophase. But there is great difference between X-ray profiles of the series of polymers at low angles. The peaks around 5.9° (2θ) is due to the scattering from the sample holder (glass tube) (26),

X-ray diffraction studies are usually carried out to obtain more detailed information on LC phase structure of LCPs. In general, a sharp and strong peak at low angle ($1^\circ < 2\theta < 4^\circ$) in small angle X-ray scattering (SAXS) curves and a broad peak in wide-angle X-ray diffraction (WAXD) curves can be observed for smectic structure. For nematic structure and cholesteric structure, no strong peak appears in SAXS but a broad peak can be observed in WAXD. For **P1** without sulfonic acid in the polymer systems, the presence of sharp and strong peak

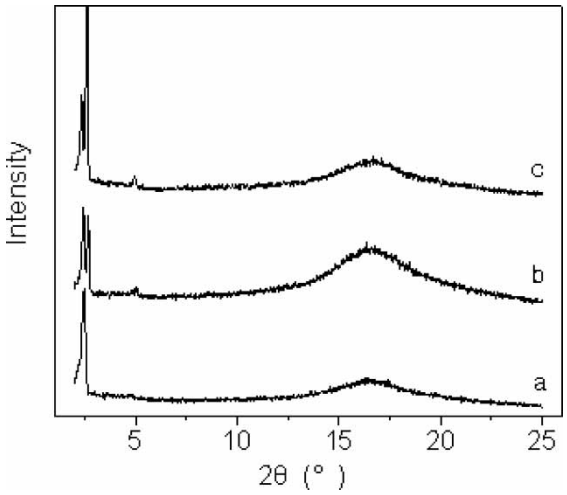

Fig. 7. X-ray profiles of series of polymers for (a) **P1**; (b) **P4** and (c) **P6**.

at low angle ($2\theta = 2.51^\circ$, corresponding to d spacing 35 Å) and a broad peak in wide-angle ($2\theta = 16.61^\circ$) clearly revealed the smectic structure of the sample. The only one strong peak at low angle indicates high-ordered lamellar structure because of homogeneous rigid moieties in the soft polymer matrix. This result agrees with DSC thermograms and optical textures analysis of **P1**. For the polymers containing more sulfonic acid in the polymer systems, two sharp peaks appeared at low angles around $2\theta = 2.5^\circ$ and 2.7°, respectively. Furthermore, the intensities of these two peaks varied with different content of sulfonic acid groups in the polymer systems. For **P3** and **P4**, the peaks around $2\theta = 2.5^\circ$ were

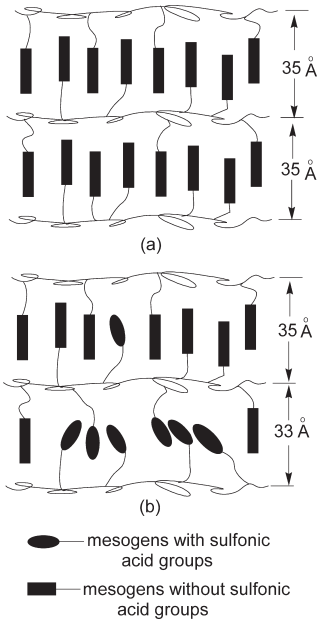

Fig. 8. Proposed structure of the polymers for (a) polymer **P1** without sulfonic groups; (b) polymers containing sulfonic groups.

stronger than those around $2\theta = 2.7^\circ$. On the contrary, the peaks around $2\theta = 2.7^\circ$ were stronger than those around $2\theta = 2.5^\circ$ for **P6** and **P7**. Besides, two peaks of polymer **P5** at low angle were in similar intensity.

These results would be interpreted by influence of H-bond derived from sulfonic acid groups in the polymer systems. When some sulfonic mesogens were introduced into the polymer systems, H-bond derived from sulfonic acids would aggregate. Withan increase of sulfonic acid mesogens in the polymer systems, the hydrogen-bonding aggregates in domains would divide the rigid mesogens into two kinds of nanophases, that is, one containing non H-bond mesogens and another involving H-bonding aggregated mesogens. These two different nanophases result in different lamellar spacings corresponding to the peak at $2\theta \approx 2.5^\circ$ (d spacing 35 Å) and $2\theta \approx 2.7^\circ$ (d spacing 33'Å), respectively. The proposed structures were displayed in Figure 8. For **P3** and **P4** containing a little sulfonic acid groups, H-bonding aggregated mesogens are lower than non H-bond mesogens, leading to a weaker peak at 27° (2θ). On the contrary, H-bonding aggregated mesogens are greater than non H-bond mesogens in **P6** and **P7**, resulting in a stronger peak at 27° (2θ).

4 Conclusions

The polysiloxanes synthesized with cholesteryl 6-undec-10-enoyloxy-naphthalene-2-carboxylate (**M1**) and cholesteryl 3-sulfo-4-undec-10-enoyloxy-benzoate (**M2**) were prepared in a one-step reaction with sulfonic acid group contents ranging between 0 and wt 4.39%. On heating and cooling cycles, the monomer **M1** showed cholesteric mesophase, while **M2** exhibited cholesteric and smectic phase. In comparison with a long pitch structure of **M1,** the cholesteric phase of **M2** suggests a short pitch structure due to H-bonding interaction derived from sulfonic acid groups. All the polymers **P1** ~ **P7** displayed smectic mesophase.

With an increase of sulfonic acid groups in the polymers, the glass transition temperature rose slightly; while the temperature of clear point decreased, leading to a mesophase temperature ranges decrease. For polysiloxanes, the glass-transition temperature may be considered as a measure of the backbone flexibility. In our case, the backbone flexibility of the polymers is influenced mainly by H-bonding interaction derived sulfonic acid groups. As sulfonic groups increased in the polymer systems, H-bonding interaction strengthened, resulting in an increase of glass transition temperature. On the other hand, when some sulfonic mesogens were introduced into the polymer systems, H-bond derived from sulfonic acids would aggregate, thus the homogeneous rigid moieties and the high-ordered lamellar structure would be destroyed, resulting in T_i decreased.

In X-ray measurement, all the polymers displayed sharp strong peaks and broad peaks at low angle around $2\theta \approx 2.6^\circ$ and wide-angle around $2\theta \approx 16.6^\circ$, respectively. The broad peaks of all the polymers appeared around $2\theta \approx 16.6^\circ$ are similar, but there is great difference between X-ray profiles of the series of polymers at low angles. For **P1** without sulfonic acid in the polymer systems, the presence of sharp and strong peak at low angle ($2\theta = 2.51^\circ$, corresponding to d spacing 35 Å) revealed clearly the smectic structure of the sample. The only one strong peak at low angle indicates high-ordered lamellar structure because of homogeneous rigid moieties in the soft polymer matrix. For the polymers containing more sulfonic acid in the polymer systems, two sharp peaks appeared at low angles around $2\theta = 2.5^\circ$ and 2.7°, respectively. Furthermore, the intensities of these two peaks varied with different content of sulfonic acid groups in the polymer systems. For **P3** and **P4**, the peaks around $2\theta = 2.5^\circ$ were stronger than those around $2\theta = 2.7^\circ$. On the contrary, the peaks around $2\theta = 2.7^\circ$ were stronger than those around $2\theta = 2.5^\circ$ for **P6** and **P7**. With an increase of sulfonic acid mesogens in the polymer systems, the hydrogen-bonding aggregates in domains would divide the rigid mesogens into two kinds of nanophases, that is, one containing non H-bond mesogens and another involving H-bonding aggregated mesogens. These two different nanophases result in different lamellar spacings.

5 Acknowledgments

The authors are grateful to the National Natural Science Fundamental Committee of China, HI-Tech Research and Development Program (863) of China, National Basic Research Priorities Program (973) of China, and the Science and Technology Department of Liaoning Province for financial support of this work.

6 References

1. Lin, H.C. and Hendrianto, J. (2005) *Polymer*, **46**, 12146–12157.
2. Kawakami, T. and Kato, T. (1998) *Macromolecules*, **31**, 4475–4479.
3. Martin, S.M. and Ward, M.D. (2005) *Langmuir*, **21**, 5324–5331.
4. Sivakova, S., Bohnsack, D.A. and Mackay, M.E. (2005) *J. Amer. Chem. Soc.*, **127**, 18202–18211.
5. Nair, K.P., Pollino, J.M. and Weck, M. (2006) *Macromolecules*, **39**, 931–940.
6. Lu, X., He, C., Terrell, C.D. and Griffin, A.C. (2002) *Macromol. Chem. Phys.*, **203**, 85–88.
7. Sasaki, T. and Fukunaga, G. (2005) *Chem. Mater.*, **17**, 3433–3438.
8. Medvedev, A.V., Barmatov, E.B., Medvedev, A.S., Shibaev, V.P., Ivanov, S.A., Kozlovsky, M. and Stumpe, J. (2005) *Macromolecules*, **38**, 2223–2229.

9. Burke, K.A., Sivakova, S., Mckenzie, B.M., Mather, P.T. and Rowan, S.J. (2006) *J. Polym. Sci. Part A: Polym. Chem.*, **44**, 5049–5059.
10. Cui, L. and Zhao, Y. (2004) *Chem. Mater.*, **16**, 2076–2082.
11. Kato, T. and Frechet, J.M. (1995) *J. Macromol. Symp.*, **98**, 311–326.
12. Fouquey, C., Lehn, J.M. and Levelut, A.M. (1990) *Adv. Mater.*, **2**, 254–258.
13. Malik, S., Dhal, P.K. and Mashelkar, R.A. (1995) *Macromolecules*, **28**, 2159–2164.
14. Gray, G.W. and Jones, B. (1953) *J. Chem. Soc.*, 4179–4188.
15. Gray, G.W. and Jones, B. *Molecular Structure and Liquid Crystals*; Academic Press: London, 61–63, 1967.
16. Jeffrey, G.A. and Wingert, L.M. (1992) *Liq. Cryst.*, **12**, 179–185.
17. Frank, H., Carsten, T. and Horst, Z. (1991) *Angew. Chem., Int. Ed. Eng.*, **30**, 440–447.
18. Gohy, J.F., Sobry, R., Bossche, G.V. and Jerome, R. (2000) *Polym. Int.*, **49**, 1293–1301.
19. Malik, S., Dhal, P.K. and Mashelkar, R.A. (1995) *Macromolecules*, **28**, 2159–2166.
20. Martin, S.M., Yonezawa, J., Horner, M.J., Macosko, C.W. and Ward, M.D. (2004) *Chem. Mater.*, **16**, 3045–3055.
21. Zhang, B.Y., Meng, F.B., Li, Q.Y. and Tian, M. (2007) *Langmuir*, **23**, 6385–6390.
22. Zhang, B.Y., Meng, F.B., Zang, B.L. and Hu, J.S. (2003) *Macromolecules*, **36**, 3320–3326.
23. Chow, K.S. and Khor, E. (1998) *Adv. Chitin. Sci.*, **3**, 147–152.
24. Dierking, I. *Textures of Liquid Crystals*; Wiley-VCH: Weinheim, 56–64, 2003.
25. Graiver, D., Litt, M. and Baer, E. (1979) *J. Polym. Sci., Polym. Chem.*, **17**, 3573–3587.
26. Xu, J., Toh, C.L., Liu, X., Wang, S., He, C. and Lu, X. (2005) *Macromolecules*, **38**, 1684–1690.